Received: 9 October 2023 | Revised: 25 December 2023 | Accepted: 8 January 2024

DOI: 10.1111/ejn.16261

RESEARCH REPORT

EJN European Journal of Neuroscience FENS WILEY

# Classification of Alzheimer's disease: application of a transfer learning deep Q-network method

**Huibin Ma**[1,2] | **Yadan Wang**[1,2] | **Zeqi Hao**[3] | **Yang Yu**[4] | **Xize Jia**[5] | **Mengting Li**[3] | **Lanfen Chen**[6]

[1]School of Information and Electronics Technology, Jiamusi University, Jiamusi, China

[2]Key Laboratory of Autonomous Intelligence and Information Processing in Heilongjiang Province, Jiamusi, China

[3]School of Psychology, Zhejiang Normal University, Jinhua, China

[4]Department of Psychiatry, the second affiliated hospital of Zhejiang University school of Medicine, Zhejiang, China

[5]Department of Radiology, Changshu No. 2 People's Hospital, The Affiliated Changshu Hospital of Xuzhou Medical University, Changshu, China

[6]School of Medical Imaging, Weifang Medical University, Weifang, China

**Correspondence**
Lanfen Chen, School of Medical Imaging, Weifang Medical University, Weifang, China.
Email: chenlanfen@wfmc.edu.cn

Mengting Li, School of Psychology, Zhejiang Normal University, Jinhua, China.
Email: limengting1108@zjnu.edu.cn

**Funding information**
National Natural Science Foundation of China, Grant/Award Numbers: 82001898, 82001896

Edited by: Yoland Smith

## Abstract

Early diagnosis is crucial to slowing the progression of Alzheimer's disease (AD), so it is urgent to find an effective diagnostic method for AD. This study intended to investigate whether the transfer learning approach of deep Q-network (DQN) could effectively distinguish AD patients using local metrics of resting-state functional magnetic resonance imaging (rs-fMRI) as features. This study included 1310 subjects from the Consortium for Reliability and Reproducibility (CoRR) and 50 subjects from the Alzheimer's Disease Neuroimaging Initiative (ADNI) GO/2. The amplitude of low-frequency fluctuation (ALFF), fractional ALFF (fALFF) and percent amplitude of fluctuation (PerAF) were extracted as features using the Power 264 atlas. Based on gender bias in AD, we searched for transferable similar parts between the CoRR feature matrix and the ADNI feature matrix, resulting in the CoRR similar feature matrix served as the source domain and the ADNI similar feature matrix served as the target domain. A DQN classifier was pre-trained in the source domain and transferred to the target domain. Finally, the transferred DQN classifier was used to classify AD and healthy controls (HC). A permutation test was performed. The DQN transfer learning achieved a classification accuracy of 86.66% ($p < 0.01$), recall of 83.33% and precision of 83.33%. The findings suggested that the transfer learning approach using DQN could be an

**Abbreviations:** AD, Alzheimer's disease; ADNI, Alzheimer's Disease Neuroimaging Initiative; ALFF, amplitude of low-frequency fluctuation; AUC, area under the receiver operating characterization curve; CNN, convolutional neural networks; CoRR, Consortium for Reliability and Reproducibility; DNN, deep neural networks; DQN, deep Q-network; EMD, Earth mover's distance; fALFF, fractional amplitude of low-frequency fluctuation; GNB, Gaussian naive Bayes; GNN, graph neural networks; HC, healthy controls; LR, logistic regression; LSTM, long short-term memory networks; PerAF, percent amplitude of fluctuation; ROC, receiver operating characterization; ROIs, regions of interest; SVM, support vector machine.

Huibin Ma and Yadan Wang have contributed equally to this work and share first-authorship.

effective way to distinguish AD from HC. It also revealed the potential value of local brain activity in AD clinical diagnosis.

**KEYWORDS**
Alzheimer's disease, deep Q-network, local metrics, reinforcement learning, resting-state fMRI, transfer learning

## 1 | INTRODUCTION

Alzheimer's disease (AD) is a progressive neurodegenerative disorder characterized by impaired memory, difficulty learning and thinking, and uncontrolled behaviour, placing a heavy burden on families and caregivers (Bondi et al., 2017). However, the etiological factors of AD are complex, and the diagnosis is challenging (Breijyeh & Karaman, 2020). In clinical practice, there is an urgent need to discover effective methods for diagnosing AD.

Existing research has confirmed brain dysfunction in AD patients by using resting state functional magnetic resonance imaging (rs-fMRI) (Bi et al., 2019, 2020; Li et al., 2017). Based on the objective neuromarkers detected by rs-fMRI, studies attempted to combine rs-fMRI with machine learning algorithms to achieve accurate diagnosis of AD. For example, scholars applied support vector machine (SVM) to classify AD patients based on brain functional connectivity features, of which the total accuracy rate reached 81.22% (Zhao et al., 2019). Convolutional neural networks (CNN) and long short-term memory networks (LSTM) were also used for AD classification, achieving an accuracy rate of 91.43% (Noh et al., 2023). Another study used local graph neural networks (GNN) to obtain local biomarkers and then used global GNN to learn the relationship between subjects and local biomarkers, achieving an accuracy of 82.09% for AD classification (Zhang et al., 2022). However, most fMRI studies face the limitation of small sample sizes, which brings issues of overfitting and weak generalization in machine learning studies (Bi et al., 2018; Li et al., 2022; Yosinski et al., 2014).

Transfer learning is a machine learning method that concentrates on knowledge transfer between domains. The classifier of transfer learning is pre-trained on a large-scale dataset in the source domain and then fine-tuned on a small-scale dataset in the target domain, resulting in higher accuracy and addressing overfitting and weak generalization issues in small-scale data (Yosinski et al., 2014). Transfer learning has been successfully applied in distinguishing obsessive–compulsive disorder (Kalmady et al., 2021), attention-deficit/hyperactivity disorder (Meng et al., 2022) and autism (Gao et al., 2021). For example, researchers utilized brain connectivity of AD patients as features and employed graph CNN for transfer learning to identify AD. This approach achieved a classification accuracy of 89.4% (Li et al., 2021). In a study on diagnosing patients with mild cognitive impairment (MCI), which is associated with an increased risk of developing AD, transfer learning has achieved an accuracy rate of 82.4% (Li et al., 2019). From the brain connectivity or network perspective, the effectiveness of transfer learning in AD classification has been revealed. However, whether the local brain activity of AD patients can serve as a feature for transfer learning remains to be explored.

To characterize local spontaneous neural brain activity, several rs-fMRI methods have been proposed. The amplitude of low-frequency fluctuation (ALFF) is a reliable indicator for detecting the intensity of spontaneous activity in the brain (Yu-Feng et al., 2007). Based on ALFF, the fractional ALFF (fALFF) is obtained by the ratio of low-frequency power spectrum to the power across the entire frequency range, which provides a more sensitive and specific measure for detecting spontaneous brain activity (Zou et al., 2008). And the percent amplitude of fluctuation (PerAF) is a scale-independent method that is not influenced by the scale of the original signal, which shows higher reliability (Jia et al., 2020). The combination of the three metrics could comprehensively explore the brain activity characteristics of AD at single voxel level.

Overall, there are few studies using rs-fMRI for AD transfer learning, and few scholars who directly utilize local metrics for transfer learning. Therefore, this study proposed a transfer learning method based on the transfer deep Q-network (DQN), which utilized local abnormalities of AD patients as features and employed a DQN for model parameter transfer learning.

## 2 | MATERIALS AND METHODS

### 2.1 | Participants

The source domain samples for this study came from Consortium for Reliability and Reproducibility (CoRR). There are 33 datasets in total, of which 32 datasets are available

for download. Prior to the data collection, all researchers confirmed that it was collected with the approval of local ethics committee or institutional review board and that the data were shared through CoRR. The 32 downloadable datasets consist of 19 data sites, which were divided into 36 groups based on time points and slice quantities. Subjects were divided into two groups according to gender, with 653 male and 657 female subjects. Inclusion criteria included (1) subjects with corresponding T1 images; (2) images with good normalization effect; (3) subjects without excessive head movements (translations or rotations should be less than 3 mm or 3°); and (4) exclusion of non-right-handed subjects. Diagnostic information, ethical statements, and scanning information for all scanners are available at https://fcon_1000.projects.nitrc.org/indi/CoRR/html/samples.html. The target domain samples for this experiment were obtained from ADNI GO/2 and included all baseline AD and healthy control (HC) rs-fMRI data. Subjects were divided into two groups, AD and HC. Twenty-five subjects were included in the AD data, of which six AD subjects were from Apoe3 and 19 AD subjects were from Apoe4. Twenty-five subjects were included in the HC data, of which 17 HC subjects were from Apoe3 and eight HC subjects were from Apoe4. Criteria for inclusion included (1) subjects with corresponding T1 images; (2) images with good normalization effect; (2) subjects without large head movements (translations or rotation less than 3 mm or 3°); (3) exclusion of non-right-handed subjects; and (4) by matching the age and gender with the AD group, 25 HC subjects were selected as the control group. Diagnostic information about the scanner and information about the scan can be found at https://adni.loni.usc.edu/. The status of the included CORR and ADNI data was shown in Table 1.

## 2.2 | Resting-state fMRI data preprocessing

The same preprocessing steps are applied for CoRR and ADNI data. The software packages used for data preprocessing were RESTplus V1.25 (Jia et al., 2019) and the Statistical Parameter Mapping tool (SPM12) based on MATLAB 2017b platform. The specific preprocessing steps were (1) removal of the first 10 time points; (2) slice-timing correction; (3) head-motion correction; (4) spatial normalization and resampling into voxels of $3 \times 3 \times 3$ size; (5) spatial smoothing with a half-height full-width (FWHM) of [6 6 6]; (6) removal of the linear drift in the time course; (7) nuisance covariate regression based on the Frison-24 parameters (Friston et al., 1996); and (8) for PerAF calculation, bandpass filtering was performed with a frequency range of 0.01–0.08 Hz.

## 2.3 | Indicator calculation and feature extraction

Rs-fMRI data of CoRR and ADNI datasets were processed in the same way. ALFF, fALFF and PerAF metrics were calculated using RESTplus V1.25. The calculation process of ALFF was as follows: The fast Fourier transform (FFT), first of all, was applied to the pre-processed data, which transformed the rs-fMRI signal from time domain to frequency domain, thus obtaining the power spectrum. In the range of 0.01–0.08 Hz, the square root at each frequency was obtained, and the square root was averaged to obtain ALFF. The ALFF calculation process includes bandpass filter (0.01–0.08 Hz). Thus, for ALFF calculation, filter was not conducted during preprocessing (Yu-Feng et al., 2007). The calculation process of fALFF was as follows: First, the time series of each voxel was transformed into the frequency domain. Then, the square root was calculated for each frequency in the power spectrum. To obtain fALFF, the sum of amplitudes in the frequency range of 0.01–0.08 Hz was divided by the sum of amplitudes across the entire frequency range. For fALFF calculation, the sum of amplitudes in the entire frequency band (0.01–0.25 Hz) was needed. Thus, filter was not conducted for the fALFF

**TABLE 1** Demographics and clinical characteristics of all subjects.

| | CoRR | | ADNI | | |
|---|---|---|---|---|---|
| **Measure** | **HC ($n = 1310$) Mean (SD)** | ***p*-value** | **HC ($n = 25$) Mean (SD)** | **AD ($n = 25$) Mean (SD)** | ***p*-value** |
| Age (years) | 25.47 (14.89) | 0.42[a] | 73.75 (4.9) | 72.28 (6.98) | 0.40[a] |
| Sex(M/F) | 653/657 | — | 11/14 | 13/12 | 0.57[b] |

Abbreviations: AD, Alzheimer's disease; ADNI, Alzheimer's Disease Neuroimaging Initiative; CoRR, Consortium for Reliability and Reproducibility; F, female; HC, Healthy Controls; M, male.

[a]The *p*-value was obtained by Student's *t*-test.

[b]The *p*-value was obtained by two-tailed Pearson chi-square *t*-test.

calculation (Zou et al., 2008). PerAF was calculated by the following formula (Jia et al., 2020):

$$\mathrm{PerAF} = \frac{1}{n}\sum_{i=1}^{n}\left|\frac{x_i - \mu}{\mu}\right| \times 100\%$$

where $n$ is the number of time points in a single voxel time series, $x_i$ is the signal intensity at the $i$th time point on the single voxel time series and $\mu$ is the signal mean of the single voxel time series.

For standardization, the ALFF of each voxel was normalized by dividing it by the average ALFF of the entire brain. Similarly, fALFF and PerAF were also standardized using the same approach. Then, mALFF, mfALFF and mPerAF were obtained, respectively.

The Power 264 atlas was used to segment the brain region into 264 regions of interest (ROIs) which were used to extract metrics for mALFF, mfALFF and mPerAF, respectively. Seven hundred and ninety-two features were extracted from the CoRR data, of which 264 features were extracted from mALFF, 264 features were extracted from mfALFF and 264 features were extracted from mPerAF. The ADNI data also obtained 792 features with same compositions as these in the CoRR dataset. Two feature matrices were obtained: CoRR feature matrix and ADNI feature matrix, of which the sizes were the number of subjects × 792 in each dataset.

## 2.4 | Transfer learning

First, this study conducted preliminary screening of subjects, selecting similar subjects from CoRR to find potential transferable components. According to the gender bias of AD, the prevalence of AD is higher in females than in males (Subramaniapillai et al., 2021). This study calculated the mean signal of AD and HC separately, with the dimension of the mean signal being 1 × 792. The cosine distance between the mean signal of AD and female subjects as well as that between the mean signal of HC and male subjects in CoRR were measured. Cosine distance only considers the similarity in direction of values and is not affected by the magnitude of values, so it is suitable for preliminary screening of subjects (Kirişci, 2023). We selected a fixed number of female subjects with the closest cosine distance to AD and a fixed number of male subjects with the closest cosine distance to HC. On this basis, a new CoRR feature matrix was constructed.

Next, the screening of similar features was conducted to further identify transferable parts and prepare for transfer learning. The Earth mover's distance (EMD) and Sinkhorn combination algorithm were used to measure the distance between two features with same location in the new CoRR feature matrix and ADNI feature matrix by using coupling matrices (Gautheron et al., 2019). Then, a ranking of feature similarity was obtained, and a fixed number of most similar features were selected by employing the EMD and Sinkhorn combination algorithms. Based on the new CoRR feature matrix, ADNI similar feature matrix and CoRR similar feature matrix were constructed.

Finally, in this study, transfer learning was conducted using the DQN as the base model. The large-sample CoRR similar feature matrix was used as the source domain, and the small-sample ADNI similar feature matrix was used as the target domain. First, the DQN classifier was pre-trained using the source domain data. The parameters used during the learning process of the pre-trained model can be found in the supplementary material (Table S2 in the Supporting Information). The pre-trained local and target network parameters in the source domain DQN models were transferred to the local and target network of the target domain DQN model as the initial parameters. The target domain dataset was divided into a training set and a test set in a ratio of 7:3. Transfer learning with DQN was performed using the target domain training set. Due to the limited number of subjects, leave-one-out cross-validation was used for parameter tuning. When there were 300 similar male subjects and 300 similar female subjects in the source domain, as well as 170 similar features, the target domain DQN model achieved good results, as shown in the results table in the Supporting Information (Table S1). After parameter tuning on the training set, the best set of parameters was found, which was considered the optimal model. The specific model parameters can be found in the target domain DQN model parameter table in the supplementary materials (Table S3 in the Supporting Information). To test the effectiveness of the optimal model, the target domain test set was used for evaluation. Permutation test was used in this study to evaluate the statistical significance of prediction accuracy (Golland & Fischl, 2003). The labels in the training and test sets were randomly shuffled, and the shuffled training and test sets were trained and predicted using the optimal parameter model obtained before. This process was repeated 5000 times in total. The accuracy obtained from the 5000 experimental runs was compared with the original accuracy. The number of times that the accuracy was greater than or equal to the original test set accuracy was counted and divided by the total number of permutations. If the $p$-value is less than 0.05, the original accuracy is considered significant (Zhao

et al., 2022). The specific process of the transfer learning algorithm is shown in Figure 1.

## 2.5 | Classification with other algorithms

We applied DQN, SVM, logistic regression (LR) and Gaussian naive Bayes (GNB) for the classification of AD in the ADNI dataset. Due to high dimensionality of the small sample features, Lasso was used for feature selection. In the comparative algorithms, the optimal parameters and classifier models were obtained based on the leave-one-out cross-validation results of the target domain training set. The optimal classifier model was evaluated using the target domain test set. In the SVM algorithm, a linear kernel function was used with a $C$ parameter set to 0.1, and 31 features were selected. In the LR algorithm, L2 regularization was used with a regularization strength parameter $C$ set to 0.4, and 57 features were selected. The GNB classifier selected 13 features. The model

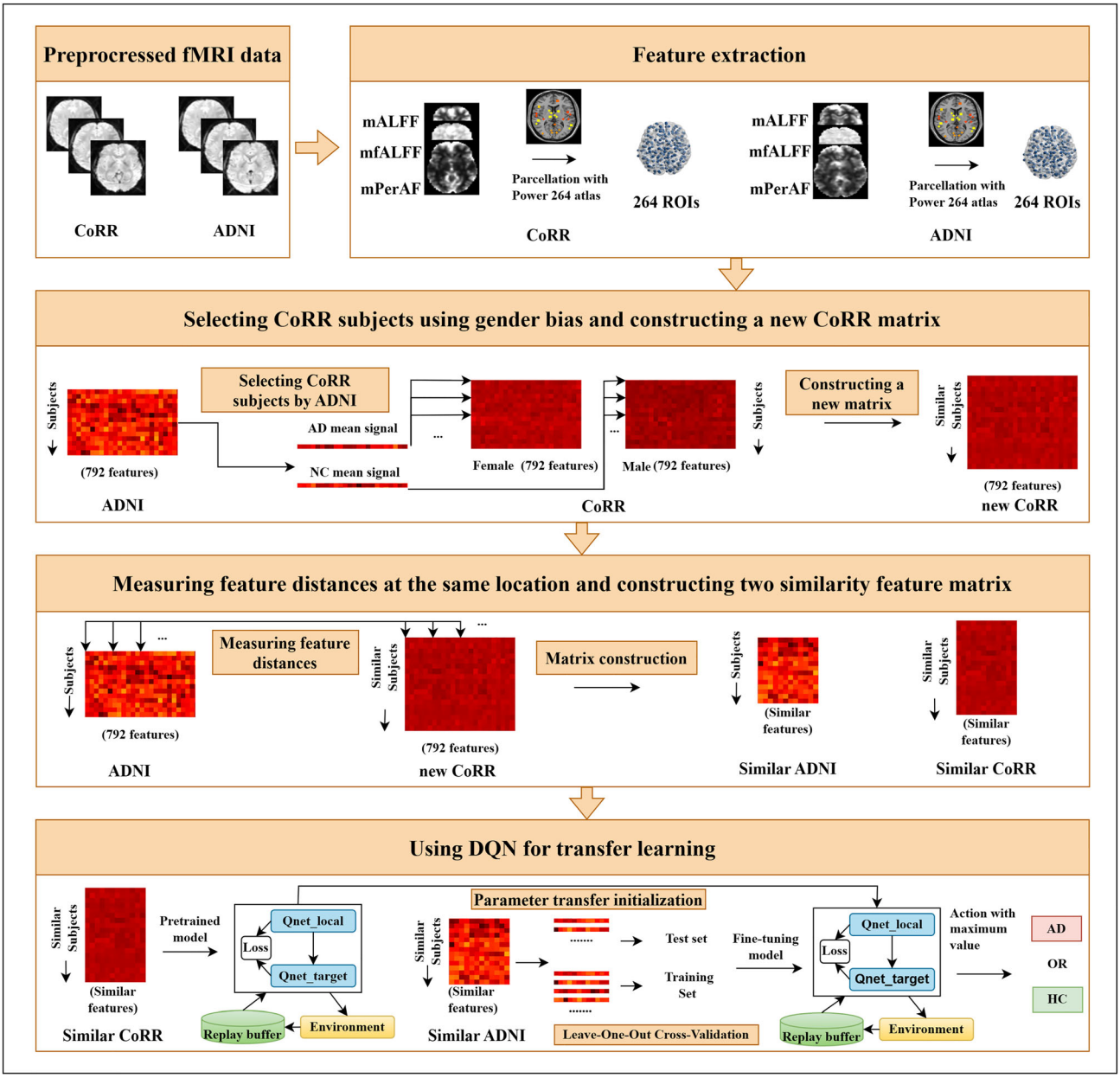


FIGURE 1 Process of transfer learning. AD, Alzheimer's disease; ADNI, Alzheimer's disease neuroimaging initiative; CoRR, consortium for reliability and reproducibility; DQN, deep Q-network; HC, healthy controls; similar ADNI, ADNI similar feature matrix; similar CoRR, CoRR similar feature matrix.

**TABLE 2** Comparison of results of different algorithms.

| Method | Similar subjects | Similar features | Accuracy (%) | Recall (%) | Precision (%) | AUC |
|---|---|---|---|---|---|---|
| TL-DQN | 300 × 2 | 170 | 86.66 | 83.33 | 83.33 | 0.87 |
| DQN | — | — | 60 | 66.66 | 50 | 0.62 |
| SVM | — | — | 73.33 | 66.66 | 66.66 | 0.83 |
| LR | — | — | 80 | 83.33 | 71.42 | 0.85 |
| GNB | — | — | 73.33 | 66.66 | 66.66 | 0.81 |

Abbreviations: AUC, area under the receiver operating characteristic curve; DQN, deep Q-network; GNB, Gaussian naïve Bayes; LR, logistic regression; SVM, support vector machine; TL-DQN, transfer learning with deep Q-network.

parameters for the DQN classifier can be found in Table S4.

## 3 | RESULTS

### 3.1 | Demographic information

In the CoRR dataset, 45 subjects were excluded due to missing structural magnetic resonance imaging; 59 subjects were excluded due to poor normalization quality; 61 subjects were excluded due to excessive head motion (translation or rotation greater than 3 mm or 3°), and 14 subjects were excluded because they were not right-handed. Finally, a total of 1310 subjects were included in this study, including 653 males and 657 females. In the ADNI dataset, nine subjects were excluded due to original data missing, two subjects were excluded due to excessive head motion (translation or rotation greater than 3 mm or 3°), two subjects were excluded due to non-right-handedness, and 11 HC were excluded due to advanced age and gender mismatch. Finally, 50 subjects were included in the study, including 25 AD patients and 25 HC (Table 1).

### 3.2 | Classification results of different algorithms

Table 2 presents a comparison between the transferred DQN classifier and other classifiers. We selected 300 × 2 similar subjects from CoRR and extracted the top 170 similar features to construct the CoRR similar feature matrix (600 × 170) and the ADNI similar feature matrix. After transfer learning, the classification accuracy reached 86.66%. The recall rate was 83.33%. The precision was 83.33%. And the area under the receiver operating characteristic (ROC) curve was 0.87. Table 2 demonstrates that when the number of similar features was 170, transfer learning with DQN performed better than other methods. The table provides a comparison of the results

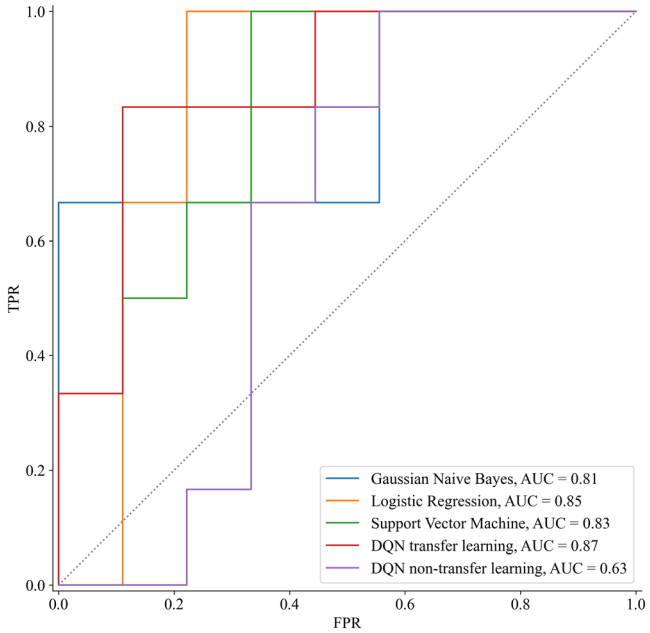


**FIGURE 2** Receiver operating characterization (ROC) curve for metrics from multiple classifiers. The image of ROC was displayed using the Matplotlib toolkit in python. AUC, area under the ROC curve; FPR, false positivity rate; TPR, true positivity rate.

for classifying ADNI subjects directly using the DQN classifier, showing significantly improved results after transfer. The ROC curve in Figure 2 shows that the classifier in this study outperformed other methods at the point where the number of similar features was 170. Figure 3 depicts the results of performing 5000 permutation tests, which further investigated whether the prediction results were merely accidental. The calculated *p*-value was less than 0.01, indicating that the accuracy obtained from the real data was significantly higher than that generated randomly.

## 4 | DISCUSSION

Studies on medical imaging usually have small sample sizes. However, in machine learning, a small number of

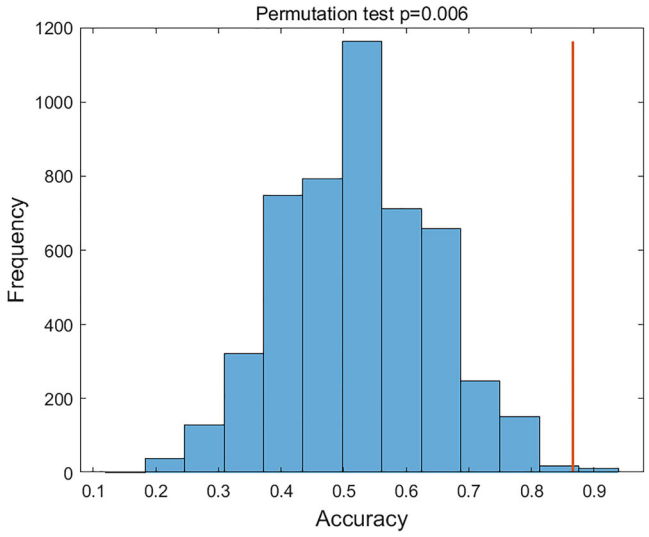


**FIGURE 3** The results of performing 5000 permutation tests.

subjects can cause problems such as overfitting, leading to biased machine learning (Vabalas et al., 2019). Therefore, this study provided a reference framework that used a medical image database with low similarity and transfer learning to alleviate issues such as overfitting and weak generalization ability. Based on the local brain activities, the results showed that using transfer learning with a DQN can successfully classify AD and HC with the final classification accuracy of 86.66%, the recall rate of 83.33%, the precision of 83.33% and the AUC of 0.87.

Firstly, many AD classification methods are limited to the feature information of small samples. For example, some scholars fused brain region information and genetic information as features and use the method of clustering random forest for AD classification (Bi et al., 2020). Some researchers integrated cortical features to classify AD (de Vos et al., 2016). Some researchers combined texture features of brain imaging with clinical features to classify AD (Altaf et al., 2018). The fusion of features can, to some extent, alleviate the overfitting problem in small-sample machine learning. However, the feature information is also limited by the small sample size itself. Our study utilized a large-sample CoRR dataset, which allowed us to expand the scope beyond the limitations of small-sample feature information.

Secondly, we applied a novel transfer learning method based on DQN, which not only identified transferable parts in CoRR and ADNI datasets but also utilized adaptive deep reinforcement learning algorithms. Compared with traditional methods such as SVM, the most used classifier for small-sample medical imaging data classification (LaConte et al., 2005; Steardo et al., 2020; Wang et al., 2007), deep reinforcement learning algorithms have stronger robustness and generalization ability. They can effectively address the challenges posed by small-sample problems when combined with transfer learning. Compared to other deep models such as CNN (Qureshi et al., 2019) and deep neural networks (DNN) (Yang et al., 2020), the DQN model relies on rewards to drive its learning process, and the learning is influenced by the reward scores (Mnih et al., 2015). This approach helps to mitigate issues arising from differences in label information between the source and target domains. In the CoRR and ADNI databases used in this study, the labels are inconsistent and have low similarity. The transfer learning method based on DQN can overcome these issues and achieve higher accuracy.

The local indicators of resting-state brain imaging have always been the focus of researchers. In previous studies, researchers have used local metrics to conduct extensive research on resting-state brain imaging (Chen et al., 2022; Wu et al., 2021). In this study, we used a combination of local indicators including ALFF, fALFF and PerAF for the first time to study AD. The experimental results showed that the combination of the three local metrics can serve as effective biomarkers in identifying AD.

Local indicators can accurately locate specific brain regions and identify distinctive characteristics of those regions. In non-machine learning studies of AD, some researchers found abnormalities in the ALFF indicator in certain brain regions of AD patients (Lai et al., 2022), while others discovered abnormalities in the fALFF indicator in certain brain regions (Li et al., 2017). It can be seen that previous research demonstrated that local indicators in AD patients are abnormal in certain brain regions and can be localized to specific areas. However, in current machine learning research, only a few studies used local indicators to investigate the classification of AD patients. Some scholars used ALFF as a feature and input it into an LR classifier for classification (de Vos et al., 2018). Some scholars used both ALFF and ReHo as features and input them into an SVM classifier for classification (Long et al., 2016). This study expanded the existing research by combining ALFF, fALFF and PerAF indicators. The research results confirmed that the three local indicators can serve as effective biomarkers to differentiate between AD and HC.

The combination of transferring DQN and local indicators can effectively differentiate between AD and HC, bringing important exploratory significance to the clinical diagnosis of AD. Currently, the use of machine learning for automated diagnosis of AD is still in its early stage. This study achieved good classification results and provided a preliminary exploration for automated diagnosis of AD, which has positive implications for addressing the growing need for clinical diagnostic of AD.

## 5 | CONCLUSION

Our research preliminarily demonstrated that transfer learning could successfully distinguish AD patients from HC using local brain activity as features. This provides important evidence for understanding the neuropathology of AD and strongly supports the hypothesis that local metrics have potential value in clinical diagnosis.

## AUTHOR CONTRIBUTIONS

Mengting Li, Huibin Ma and Yadan Wang conceived and designed this study. Yadan Wang executed the data analysis and wrote the first manuscript. Mengting Li, Zeqi Hao, Yang Yu, Xize Jia and Lanfen Chen helped coordinate the study and revised the manuscript. All authors have made significant scientific contributions to this article and reviewed the article.

## ACKNOWLEDGEMENTS

The authors express gratitude to the researchers who share their available data on the CoRR website and ADNI website, as well as all the researchers involved in this study.

## CONFLICT OF INTEREST STATEMENT

The authors declared that this research has no financial conflicts of interest.

## PEER REVIEW

The peer review history for this article is available at https://www.webofscience.com/api/gateway/wos/peer-review/10.1111/ejn.16261.

## DATA AVAILABILITY STATEMENT

The functional magnetic resonance imaging data used in this study is from the Consortium for Reliability and Reproducibility (http://fcon_1000.projects.nitrc.org/indi/CoRR/html/samples.html) public database and the Alzheimer's Disease Neuroimaging Initiative (https://adni.loni.usc.edu/) public database.

## ORCID

*Xize Jia* https://orcid.org/0000-0003-4698-8723

## REFERENCES

Altaf, T., Anwar, S. M., Gul, N., Majeed, M. N., & Majid, M. (2018). Multi-class Alzheimer's disease classification using image and clinical features. *Biomedical Signal Processing and Control*, *43*, 64–74. https://doi.org/10.1016/j.bspc.2018.02.019

Bi, X.-A., Cai, R., Wang, Y., & Liu, Y. (2019). Effective diagnosis of Alzheimer's disease via multimodal fusion analysis framework. *Frontiers in Genetics*, *10*, 976. https://doi.org/10.3389/fgene.2019.00976

Bi, X.-A., Chen, J., Sun, Q., Liu, Y., Wang, Y., & Luo, X. (2018). Analysis of Asperger syndrome using genetic-evolutionary random support vector machine cluster. *Frontiers in Physiology*, *9*, 1646. https://doi.org/10.3389/fphys.2018.01646

Bi, X.-A., Hu, X., Wu, H., & Wang, Y. (2020). Multimodal data analysis of Alzheimer's disease based on clustering evolutionary random forest. *IEEE Journal of Biomedical and Health Informatics*, *24*(10), 2973–2983. https://doi.org/10.1109/JBHI.2020.2973324

Bondi, M. W., Edmonds, E. C., & Salmon, D. P. (2017). Alzheimer's disease: Past, present, and future. *Journal of the International Neuropsychological Society*, *23*(9–10), 818–831. https://doi.org/10.1017/S135561771700100X

Breijyeh, Z., & Karaman, R. (2020). Comprehensive review on Alzheimer's disease: Causes and treatment. *Molecules*, *25*(24), 5789. https://doi.org/10.3390/molecules25245789

Chen, Q., Bi, Y., Zhao, X., Lai, Y., Yan, W., Xie, L., Gao, T., Xie, S., Zeng, T., Li, J., Kuang, S., Gao, L., & Lv, Z. (2022). Regional amplitude abnormities in the major depressive disorder: A resting-state fMRI study and support vector machine analysis. *Journal of Affective Disorders*, *308*, 1–9. https://doi.org/10.1016/j.jad.2022.03.079

de Vos, F., Koini, M., Schouten, T. M., Seiler, S., van der Grond, J., Lechner, A., Schmidt, R., de Rooij, M., & Rombouts, S. A. R. B. (2018). A comprehensive analysis of resting state fMRI measures to classify individual patients with Alzheimer's disease. *NeuroImage*, *167*, 62–72. https://doi.org/10.1016/j.neuroimage.2017.11.025

de Vos, F., Schouten, T. M., Hafkemeijer, A., Dopper, E. G., van Swieten, J. C., de Rooij, M., van der Grond, J., & Rombouts, S. A. R. B. (2016). Combining multiple anatomical MRI measures improves Alzheimer's disease classification. *Human Brain Mapping*, *37*(5), 1920–1929. https://doi.org/10.1002/hbm.23147

Friston, K. J., Williams, S., Howard, R., Frackowiak, R. S., & Turner, R. (1996). Movement-related effects in fMRI time-series. *Magnetic Resonance in Medicine*, *35*, 346–355. https://doi.org/10.1002/mrm.1910350312

Gao, K., Fan, Z., Su, J., Zeng, L.-L., Shen, H., Zhu, J., & Hu, D. (2021). Deep transfer learning for cerebral cortex using area-preserving geometry mapping. *Cerebral Cortex*, *32*, 2972–2984. https://doi.org/10.1093/cercor/bhab394

Gautheron, L., Redko, I., & Lartizien, C. (2019). Feature selection for unsupervised domain adaptation using optimal transport. Paper presented at the Machine Learning and Knowledge Discovery in Databases: European Conference, ECML PKDD 2018, Dublin, Ireland, September 10–14, 2018, Proceedings, Part II 18.

Golland, P., & Fischl, B. (2003). Permutation tests for classification: Towards statistical significance in image-based studies. Paper presented at the Biennial international conference on information processing in medical imaging. https://doi.org/10.1007/978-3-540-45087-0_28

Jia, X.-Z., Sun, J.-W., Ji, G.-J., Liao, W., Lv, Y.-T., Wang, J., Wang, Z., Zhang, H., Liu, D. Q., & Zang, Y. F. (2020). Percent amplitude of fluctuation: A simple measure for resting-state fMRI signal at single voxel level. *PLoS ONE*, *15*(1), e0227021. https://doi.org/10.1371/journal.pone.0227021

Jia, X.-Z., Wang, J., Sun, H.-Y., Zhang, H., Liao, W., Wang, Z., Yan, C. G., Song, X. W., & Zang, Y. F. (2019). RESTplus: An

improved toolkit for resting-state functional magnetic resonance imaging data processing. *Science Bulletin*, *64*(14), 953–954. https://doi.org/10.1016/j.scib.2019.05.008

Noh, J.-H., Kim, J.-H., & Yang, H.-D. (2023). Classification of Alzheimer's progression using fMRI data. *Sensors*, *23*(14), 6330. https://doi.org/10.3390/s23146330

Kalmady, S. V., Paul, A. K., Narayanaswamy, J. C., Agrawal, R., Shivakumar, V., Greenshaw, A. J., & Reddy, Y. C. J. (2021). Prediction of obsessive-compulsive disorder: Importance of neurobiology-aided feature design and cross-diagnosis transfer learning. *Biological Psychiatry: Cognitive Neuroscience and Neuroimaging*, *7*, 735–746. https://doi.org/10.1016/j.bpsc.2021.12.003

Kirişci, M. (2023). New cosine similarity and distance measures for Fermatean fuzzy sets and TOPSIS approach. *Knowledge and Information Systems*, *65*(2), 855–868. https://doi.org/10.1007/s10115-022-01776-4

LaConte, S., Strother, S., Cherkassky, V., Anderson, J., & Hu, X. (2005). Support vector machines for temporal classification of block design fMRI data. *NeuroImage*, *26*(2), 317–329. https://doi.org/10.1016/j.neuroimage.2005.01.048

Lai, Z., Zhang, Q., Liang, L., Wei, Y., Duan, G., Mai, W., Zhao, L., Liu, P., & Deng, D. (2022). Efficacy and mechanism of moxibustion treatment on mild cognitive impairment patients: An fMRI study using ALFF. *Frontiers in Molecular Neuroscience*, *15*, 852882. https://doi.org/10.3389/fnmol.2022.852882

Li, L., Jiang, H., Wen, G., Cao, P., Xu, M., Liu, X., Yang, J., & Zaiane, O. (2021). TE-HI-GCN: An ensemble of transfer hierarchical graph convolutional networks for disorder diagnosis. *Neuroinformatics*, *20*, 353–375. https://doi.org/10.1007/s12021-021-09548-1

Li, W., Zhang, L., Qiao, L., & Shen, D. (2019). Toward a better estimation of functional brain network for mild cognitive impairment identification: A transfer learning view. *IEEE Journal of Biomedical and Health Informatics*, *24*(4), 1160–1168. https://doi.org/10.1109/JBHI.2019.2934230

Li, W.-K., Chen, Y.-C., Xu, X.-W., Wang, X., & Gao, X. (2022). Human-guided functional connectivity network estimation for chronic tinnitus identification: A modularity view. *IEEE Journal of Biomedical and Health Informatics*, *26*, 4849–4858. https://doi.org/10.1109/jbhi.2022.3190277

Li, Y., Jing, B., Liu, H., Li, Y., Gao, X., Li, Y., Mu, B., Yu, H., Cheng, J., Barker, P. B., Wang, H., & Han, Y. (2017). Frequency-dependent changes in the amplitude of low-frequency fluctuations in mild cognitive impairment with mild depression. *Journal of Alzheimer's Disease*, *58*(4), 1175–1187. https://doi.org/10.3233/JAD-161282

Long, Z., Jing, B., Yan, H., Dong, J., Liu, H., Mo, X., Han, Y., & Li, H. (2016). A support vector machine-based method to identify mild cognitive impairment with multi-level characteristics of magnetic resonance imaging. *Neuroscience*, *331*, 169–176. https://doi.org/10.1016/j.neuroscience.2016.06.025

Meng, X., Zhuo, W., Ge, P., Zou, B., Zhu, Y., Liu, W., & Li, X. (2022). Diagnostic model optimization method for ADHD based on brain network analysis of resting-state fMRI images and transfer learning neural network. *Frontiers in Human Neuroscience*, *16*, 1005425. https://doi.org/10.3389/fnhum.2022.1005425

Mnih, V., Kavukcuoglu, K., Silver, D., Rusu, A. A., Veness, J., Bellemare, M. G., Graves, A., Riedmiller, M., Fidjeland, A. K., Ostrovski, G., Petersen, S., Beattie, C., Sadik, A., Antonoglou, I., King, H., Kumaran, D., Wierstra, D., Legg, S., & Hassabis, D. (2015). Human-level control through deep reinforcement learning. *Nature*, *518*(7540), 529–533. https://doi.org/10.1038/nature14236

Qureshi, M. N. I., Oh, J., & Lee, B. (2019). 3D-CNN based discrimination of schizophrenia using resting-state fMRI. *Artificial Intelligence in Medicine*, *98*, 10–17. https://doi.org/10.1016/j.artmed.2019.06.003

Steardo, L. Jr., Carbone, E. A., de Filippis, R., Pisanu, C., Segura-Garcia, C., Squassina, A., de Fazio, P., & Steardo, L. (2020). Application of support vector machine on fMRI data as biomarkers in schizophrenia diagnosis: A systematic review. *Frontiers in Psychiatry*, *11*, 588. https://doi.org/10.3389/fpsyt.2020.00588

Subramaniapillai, S., Almey, A., Rajah, M. N., & Einstein, G. (2021). Sex and gender differences in cognitive and brain reserve: Implications for Alzheimer's disease in women. *Frontiers in Neuroendocrinology*, *60*, 100879. https://doi.org/10.1016/j.yfrne.2020.100879

Vabalas, A., Gowen, E., Poliakoff, E., & Casson, A. J. (2019). Machine learning algorithm validation with a limited sample size. *PLoS ONE*, *14*(11), e0224365. https://doi.org/10.1371/journal.pone.0224365

Wang, Z., Childress, A. R., Wang, J., & Detre, J. A. (2007). Support vector machine learning-based fMRI data group analysis. *NeuroImage*, *36*(4), 1139–1151. https://doi.org/10.1016/j.neuroimage.2007.03.072

Wu, D., Zhao, H., Gu, H., Han, B., Wang, Q., Man, X., Zhao, R., Liu, X., & Sun, J. (2021). The effects of rs405509 on APOEε4 non-carriers in non-demented aging. *Frontiers in Neuroscience*, *15*, 677823. https://doi.org/10.3389/fnins.2021.677823

Yang, Z., Zhuang, X., Sreenivasan, K., Mishra, V., Curran, T., & Cordes, D. (2020). A robust deep neural network for denoising task-based fMRI data: An application to working memory and episodic memory. *Medical Image Analysis*, *60*, 101622. https://doi.org/10.1016/j.media.2019.101622

Yosinski, J., Clune, J., Bengio, Y., & Lipson, H. (2014). How transferable are features in deep neural networks? *Advances in Neural Information Processing Systems*, *27*.

Yu-Feng, Z., Yong, H., Chao-Zhe, Z., Qing-Jiu, C., Man-Qiu, S., Meng, L., Li-Xia, T., Tian-Zi, J., & Yu-Feng, W. (2007). Altered baseline brain activity in children with ADHD revealed by resting-state functional MRI. *Brain and Development*, *29*(2), 83–91. https://doi.org/10.1016/j.braindev.2006.07.002

Zhang, H., Song, R., Wang, L., Zhang, L., Wang, D., Wang, C., & Zhang, W. (2022). Classification of brain disorders in rs-fMRI via local-to-global graph neural networks. *IEEE Transactions on Medical Imaging*, *42*, 444–455. https://doi.org/10.1109/tmi.2022.3219260

Zhao, J., Ding, X., Du, Y., Wang, X., & Men, G. (2019). Functional connectivity between white matter and gray matter based on fMRI for Alzheimer's disease classification. *Brain and Behavior: A Cognitive Neuroscience Perspective*, *9*(10), e01407. https://doi.org/10.1002/brb3.1407

Zhao, L., Sun, Y.-K., Xue, S.-W., Luo, H., Lu, X.-D., & Zhang, L.-H. (2022). Identifying boys with autism spectrum disorder based on whole-brain resting-state interregional functional connections using a boruta-based support vector machine approach. *Frontiers in Neuroinformatics*, *16*, 761942. https://doi.org/10.3389/fninf.2022.761942

Zou, Q.-H., Zhu, C.-Z., Yang, Y., Zuo, X.-N., Long, X.-Y., Cao, Q.-J., Wang, Y. F., & Zang, Y. F. (2008). An improved approach to detection of amplitude of low-frequency fluctuation (ALFF) for resting-state fMRI: Fractional ALFF. *Journal of Neuroscience Methods*, *172*(1), 137–141. https://doi.org/10.1016/j.jneumeth.2008.04.012

## SUPPORTING INFORMATION

Additional supporting information can be found online in the Supporting Information section at the end of this article.

**How to cite this article:** Ma, H., Wang, Y., Hao, Z., Yu, Y., Jia, X., Li, M., & Chen, L. (2024). Classification of Alzheimer's disease: application of a transfer learning deep Q-network method. *European Journal of Neuroscience*, 1–10. https://doi.org/10.1111/ejn.16261